Inorg. Chem. **2008**, *47*, 10461−10468

Inorganic Chemistry

Article

Construction of Symmetric and Asymmetric Mo/S/Cu Clusters from a Cluster Precursor $[Et_4N]_2[(edt)_2Mo_2S_2(\mu\text{-}S)_2]$ (edt = Ethanedithiolate)

Zhen-Hong Wei,[†] Hong-Xi Li,[†] Wen-Hua Zhang,[†] Zhi-Gang Ren,[†] Yong Zhang,[†] Jian-Ping Lang,[*,†,‡] and Brendan F. Abrahams[§]

College of Chemistry, Chemical Engineering and Materials Science, Suzhou University, Suzhou 215123, Jiangsu, People's Republic of China, State Key Laboratory of Organometallic Chemistry, Shanghai Institute of Organic Chemistry, Chinese Academy of Sciences, Shanghai 200032, People's Republic of China, and School of Chemistry, University of Melbourne, Victoria 3010, Australia

Received June 15, 2008

Treatment of $[Et_4N]_2[(edt)_2Mo_2S_2(\mu\text{-}S)_2]$ (**1**) (edt = ethanedithiolate) with equimolar CuBr afforded an anionic hexanuclear cluster $[Et_4N]_2[(edt)_2Mo_2(\mu\text{-}S)_3(\mu_3\text{-}S)Cu]_2 \cdot 2CH_2Cl_2$ (**2**$\cdot 2CH_2Cl_2$). On the other hand, reactions of **1** with 2 equiv of CuBr in the presence of 1,2-bis(diphenylphosphino)methane (dppm) and pyridine (Py) ligands gave rise to two neutral tetranuclear clusters $[(edt)_2Mo_2O_2(\mu\text{-}S)_2Cu_2(dppm)_2]$ (**3**) and $[(edt)_2Mo_2O(\mu_3\text{-}S)(\mu\text{-}S)_2Cu_2(Py)_4]$ (**4**), respectively. The reaction of **1** with 2 equiv of CuBr followed by the addition of a mixture of dppm and Py (molar ratio = 1:2) yielded another neutral tetranuclear cluster $[(edt)_2Mo_2(\mu\text{-}S)_2(\mu_3\text{-}S)_2Cu_2(dppm)(Py)] \cdot Py$ (**5**$\cdot$Py). Compounds **2**−**5** have been characterized by elemental analysis, UV−vis spectra, IR spectra, ^1H NMR, and X-ray analysis. The structure of the dianion of **2** can be viewed as having a $[Mo_4S_8Cu_2]$ core in which two chemically equivalent $[Mo_2(\mu\text{-}S)_3(\mu_3\text{-}S)(edt)_2Cu]^-$ anions are linked by two extra Cu−S_{edt} bonds. The molecular structure of **3** may be visualized as being built of one $[(edt)_2Mo_2X_2(\mu\text{-}S)_2]^{2-}$ dianion and one $[Cu_2(dppm)_2]^{2+}$ dication that are connected by a pair of M−μ-S_{edt} bonds. Compound **4** is formed by the affiliation of two Cu(I) atoms only at one end of the $[(edt)_2Mo_2S_2(\mu\text{-}S)_2]$ moiety, connecting with the S_t atoms and the S_{edt} atom. Cluster **5**$\cdot$Py can be viewed as being constructed from the addition of one Cu atom onto the incomplete cubanelike $[Mo_2S_4Cu]$ framework through one terminal sulfur and one edt sulfur. Among the four clusters, **3** and **4** have internal mirror symmetry or pseudo mirror symmetry, respectively, while **2** and **5** are asymmetric clusters with racemic formation.

Introduction

In the past few decades, the chemistry of the sulfido-bridged dinuclear clusters consisting of a $[M_2S_4]$ core (M = Mo, W) and various transition metals has attracted much attention mainly due to their potential applications in industrial catalytic systems[1] and the industrial hydrodesulfurization (HDS) process[2] along with their rich structural chemistry.[1−5] For example, complexes $[(dtc)_2Mo_2S_2(\mu\text{-}S)_2]$ (dtc = S_2CNEt_2)[3] and $[Cp^x{}_2Mo_2S_2(\mu\text{-}S)_2]$ (Cp^x = pentam-

---

[*] Author to whom correspondence should be addressed. E-mail: jplang@suda.edu.cn.

[†] Suzhou University.

[‡] Shanghai Institute of Organic Chemistry.

[§] University of Melbourne.

(1) (a) Hidai, M.; Kuwata, S.; Mizobe, Y. *Acc. Chem. Res.* **2000**, *33*, 46–52. (b) Kuwata, S.; Hidai, M. *Coord. Chem. Rev.* **2001**, *213*, 211–305. (c) Angelici, R. J. *Acc. Chem. Res.* **1988**, *21*, 387–384. (d) Rauchfuss, T. B. *Prog. Inorg. Chem.* **1991**, *39*, 259–329. (e) Jones, W. D.; Chin, R. M. *J. Am. Chem. Soc.* **1994**, *116*, 198–203. (f) Chianelli, R. R.; Picoraro, T. A.; Halbert, T. R.; Pan, W. H.; Stiefel, E. I. *J. Catal.* **1984**, *86*, 226–230.

(2) (a) Adams, R. D. *Chem. Rev.* **1995**, *95*, 2587–2598. (b) Bianchini, C.; Jimenez, M. V.; Meli, A.; Moneti, S.; Vizza, F.; Herrera, V.; Saanchez-Delgado, R. A. *Orgaometallics* **1995**, *14*, 2342–2342. (c) Shibahara, T. *Coord. Chem. Rev.* **1993**, *123*, 73–147. (d) Adams, R. D.; Cotton, F. A. *Catalysis by Di-and Polynuclear Metal Cluster Complexes*; Wiley-VCH: New York, 1998.

(3) (a) Müller, A.; Bhattachanryya, R. G.; Mohan, N.; Pfefferkorn, B. *Z. Anorg. Allg. Chem.* **1979**, *454*, 118–124. (b) Huneke, J. T.; Enemark, J. H. *Inorg. Chem.* **1978**, *17*, 3698–3699. (c) Kuwata, S.; Hashizume, K.; Mizobe, Y.; Hidai, M. *Organometallics* **2002**, *21*, 5401–5407. (d) Hernandez-Molina, R.; Sykes, A. G. *J. Chem. Soc., Dalton Trans.* **1999**, 3137–3148.

(4) (a) Curtis, M. D.; Druker, S. H.; Goossen, L.; Kampf, J. W. *Organometallics* **1997**, *16*, 231–235. (b) Curtis, M. D.; Druker, S. H. *J. Am. Chem. Soc.* **1997**, *119*, 1027–1036. (c) Mansour, M. A.; Curtis, M. D.; Kampf, J. W. *Organometallics* **1997**, *16*, 3363–3370. (d) Mansour, M. A.; Curtis, M. D.; Kampf, J. W. *Organometallics* **1995**, *14*, 5460–5462. (e) Curtis, M. D. *J. Cluster Sci.* **1996**, *7*, 247–262.

10.1021/ic801100g CCC: $40.75

Scheme 1. Possible Frameworks Derived from **1** and Cu(I) Ions and Different Ligands

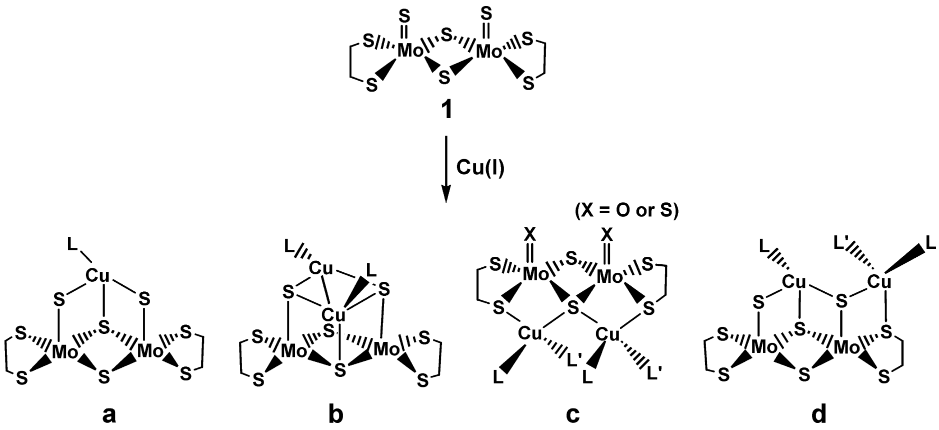

ethyl-, pentaethyl-, or pentabutyl-cyclopentadienyl)[4,5] were used as precursors to react with transition metals to form both incomplete cubanelike $[Mo_2M'S_4]$ clusters and complete cubanelike $[Mo_2M'_2S_4]$ clusters (M′ = Cu(I), Ag(I), etc). The type of cluster formed is dependent upon the ability of the terminal S_t and the bridging μ-S_{br} groups in the $[Mo_2S_4]$ core to bind further metal centers. To our knowledge, most of the clusters derived from these precursors contain a plane of symmetry. Then, how can we isolate asymmetric clusters through the introduction of M′ centers?

On the other hand, we and others have been involved in the preparation of Mo(W)/S/Cu clusters from mononuclear metal sulfide complex precursors ($[MS_4]^{2-}$, $[MOS_3]^{2-}$, and $[Cp^*MS_3]^-$ (M = Mo, W) anions).[6−9] Because most of these Mo(W)/S/Cu clusters are symmetric, we turned our attention to a $[M_2S_4]$-containing precursor, $[Et_4N]_2[(edt)_2Mo_2S_2(\mu\text{-}S)_2]$ (edt = ethanedithiolate) (**1**), that has a chelating edt at each Mo site of the $[Mo_2S_4]$ core (Scheme 1).[10] Each Mo center within this cluster is bound to three different types of sulfur atoms: the terminal sulfur (S_t), the doubly bridging sulfur (μ-S_{br}), and the chelating sulfur from edt (S_{edt}). Upon the addition of Cu(I), the S_t and μ-S_{br} atoms are usually involved in the coordination to Cu(I) centers. This has been observed in the incomplete cubanelike $[Mo_2CuS_4]$ clusters and complete cubanelike $[Mo_2Cu_2S_4]$, which are depicted as type a and type b in Scheme 1.[11] In another two examples, the μ-S_{br} and the S_{edt} atoms were also found to bind Cu(I) or Ag(I) centers, as indicated in type c (Scheme 1).[12] These results, demonstrating that the three different types of sulfur atoms, (S_{edt}, S_t, and μ-S_{br}) are capable of binding Cu(I) centers, prompted us to consider whether all three types of sulfur may be able to behave as donors in the generation of an asymmetric cluster, as depicted in type d (Scheme 1). In this paper, we describe our efforts to generate this type of cluster along with the crystal structures of **2**−**5** (Chart 1).

Results and Discussion

Synthetic and Spectral Aspects. In attempts to prepare the target cluster, we reacted **1** with CuBr. Treatment of **1** with equimolar CuBr in CH_2Cl_2/MeCN afforded a dark red solution, from which a dimeric cluster, **2**, was isolated as red crystals in 60% yield (Scheme 2). The reaction of **1** with 2 equiv of CuBr resulted in a large amount of dark red precipitate, which was found to be almost insoluble in common solvents. X-ray fluorescence analysis showed that this compound contained no bromine, while the elemental analyses of this compound for C, H, and N are quite low, suggesting it may be a large Mo/S/Cu cluster or polymer. Large Mo/S/Cu clusters are not without precedent. For

Chart 1. Designation of Compounds and Abbreviations[a] for **1**−**5**

$[Et_4N]_2[(edt)_2Mo_2S_2(\mu-S)_2]$(**1**)[10]
$[Et_4N]_2[(edt)_2Mo_2(\mu-S)_3(\mu_3-S)Cu]_2 \cdot 2CH_2Cl_2$(**2** · $2CH_2Cl_2$)
$[(edt)_2Mo_2O_2(\mu-S)_2Cu_2(dppm)_2]$ (**3**)
$[(edt)_2Mo_2O(\mu_3-S)(\mu-S)_2Cu_2(Py)_4]$ (**4**)
$[(edt)_2Mo_2(\mu-S)_2(\mu_3-S)_2Cu_2(dppm)(Py)] \cdot Py$(**5** · Py)

[a] edt = ethanedithiolate; dppm = 1,2-bis(diphenylphosphino)methane; Py = pyridine.

---

(5) (a) Halbert, T. R.; Cohen, S. A.; Stiefel, E. I. *Organometallics* **1985**, *4*, 1689–1690. (b) Kawaguchi, H.; Yamada, K.; Ohnishi, S.; Tatsumi, K. *J. Am. Chem. Soc.* **1997**, *119*, 10871–10872. (c) Brunner, H.; Janietz, N.; Wachter, J.; Zahn, T.; Ziegler, M. L. *Angew. Chem., Int. Ed.* **1985**, *24*, 133–135. (d) Ren, Z. G.; Li, H. X.; Liu, G. F.; Zhang, W. H.; Lang, J. P.; Zhang, Y.; Song, Y. L. *Organometallics* **2006**, *25*, 4351–4357.

(6) (a) Müller, A.; Dartmann, M.; Romer, C.; Clegg, W.; Sheldrick, G. M. *Angew. Chem., Int. Ed. Engl.* **1981**, *20*, 1060–1061. (b) Müller, A.; Krickemeyer, E.; Bögge, H. *Z. Anorg. Allg. Chem.* **1987**, *554*, 61–78. (c) Müller, A.; Krichemeyer, E.; Hildebrand, A.; Bögge, H.; Schneider, K.; Lemke, M. *Chem. Commun.* **1991**, 1685–1687. (d) Müller, A.; Hwang, T. K.; Bögge, H. *Angew. Chem., Int. Ed. Engl.* **1979**, *18*, 628–629. (e) Müller, A.; Bögge, H.; Schimansk, U. *Inorg. Chim. Acta* **1983**, *69*, 5–16. (f) Müller, A.; Bögge, H.; Schimansk, U. *Chem. Commun.* **1980**, 91–92. (g) Müller, A.; Diemann, E.; Jostes, R.; Bögge, H. *Angew. Chem., Int. Ed.* **1981**, *20*, 934–955.

(7) (a) Ansari, M. A.; Ibers, J. A. *Coord. Chem. Rev.* **1990**, *100*, 223–266. (b) Jeannin, Y.; Séheresse, F.; Bernés, S.; Robert, F. *Inorg. Chim. Acta* **1992**, *198*−*200*, 493–505. (c) Shi, S.; Ji, W.; Tang, S. H.; Lang, J. P.; Xin, X. Q. *J. Am. Chem. Soc.* **1994**, *116*, 3615–3616. (d) Hou, H. W.; Xin, X. Q.; Shi, S. *Coord. Chem. Rev.* **1996**, *153*, 25–56. (e) Wu, D. X.; Hong, M. C.; Cao, R.; Liu, H. Q. *Inorg. Chem.* **1996**, *35*, 1080–1082. (f) Che, C. M.; Xia, B. H.; Huang, J. S.; Chan, C. K.; Zhou, Z. Y.; Cheung, K. K. *Chem.*−*Eur. J.* **2001**, *7*, 3998–4006. (g) Zhang, Q. F.; Niu, Y. Y.; Lueng, W. H.; Song, Y. L.; Williams, I. D.; Xin, X. Q. *Chem. Commun.* **2001**, 1126–1127.

(8) (a) Shibahara, T. *Adv. Inorg. Chem.* **1991**, *37*, 143–173. (b) Arikawa, Y.; Kawaguchi, H.; Kashiwabara, K.; Tatsumi, K. *Inorg. Chem.* **2002**, *41*, 513–520. (c) Niu, Y. Y.; Zheng, H. G.; Xin, X. Q. *Coord. Chem. Rev.* **2004**, *248*, 169–183. (d) Wu, X. T. *Inorganic Assembly Chemistry*; Science Press and Science Press USA Inc.: Beijing, 2004; pp 1−179. (e) Zhang, W. J.; Behrens, A.; Gätjens, J.; Ebel, M.; Wu, X. T.; Rehder, D. *Inorg. Chem.* **2004**, *43*, 3020–3023. (f) Song, L.; Li, J. R.; Lin, P.; Li, Z. H.; Li, T.; Du, S. W.; Wu, X. T. *Inorg. Chem.* **2006**, *45*, 10155–10161. (g) Liang, K.; Zheng, H. G.; Song, Y. L.; Li, Y. Z.; Xin, X. Q. *Cryst. Growth Des.* **2007**, *7*, 373–376. (h) Zhang, C.; Song, Y. L.; Wang, X. *Coord. Chem. Rev.* **2007**, *251*, 111–141.

Scheme 2. Reactions of **1** with CuBr under the Absence or Presence of dppm and/or Py

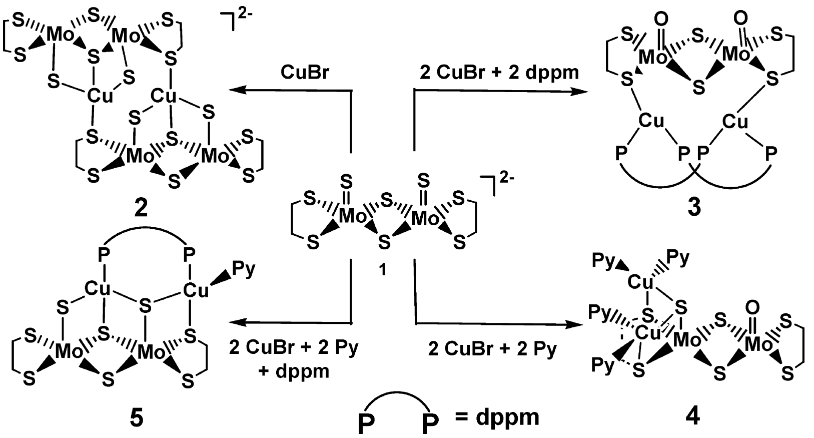

example, Wu et al. reported the isolation of a dodecanuclear cluster of composition $[Et_4N]_2[(M_2Cu_2O_2(edt)_2)_3(\mu_6\text{-}S)]$ (M = Mo, W) from the reactions of $[Et_4N]_2[M_2O_2S_2(edt)_2]$ with $Cu(NO_3)_2$ and $NaBH_4$ followed by the addition of $(NH_4)_2S_x$ solutions.[12a]

We suspected that the addition of strong donor ligands to the dark red precipitate would lead to dissolution of the solid. The strong affinity of Cu(I) for pyridine and phosphine ligands prompted us to use the ligands dppm and Py in such reactions. The addition of 2 equiv of dppm to a suspension formed by mixing **1** with 2 equiv of CuBr in MeCN led to the dissolution of the precipitate upon stirring. Upon the addition of methanol to the homogeneous red solution, red crystals of **3** were separated in 50% yield (Scheme 2). A similar reaction but with an excess of pyridine in place of the diphosphine produced **4** in 70% yield (Scheme 2). In both compounds, terminal sulfur atoms were replaced by oxygen atoms. During their preparations, such an oxidation reaction may occur in the course of crystal growth in DMF or CH_2Cl_2/MeCN/Py since the IR spectra showed a $Mo{=}S_t$ stretching vibration at 515 cm^{-1} before recrystallization and a Mo=O band at 933 cm^{-1} after recrystalization. The origin of O atoms in **3** and **4** may come from O_2 in the air or the small amount of water in the solvents used. Stiefel and his co-workers once explained the sulfur-to-oxygen transformation through a detailed theoretical analysis on the similarities and differences of the electronic structures of $[Mo_2O_2(\mu\text{-}S)_2(S_2)_2]^{2-}$ and $[Mo_2S_2(\mu\text{-}S)_2(S_2)_2]^{2-}$.[13] It is suggested that the replacement of the O atoms with S atoms leaves the higher-filled molecular orbitals (MOs) unaffected. However, the lowest unoccupied molecular orbitals (LUMOs) of Mo−S (terminal) antibonding orbits are at lower energies compared with those of Mo−O antibonding orbits. Somewhat lower activation energies should be anticipated due to the lowering of the HOMO−LUMO gap in $[Mo_2S_2(\mu\text{-}S)_2(S_2)_2]^{2-}$ compared to that in $[Mo_2O_2(\mu\text{-}S)_2(S_2)_2]^{2-}$ (HOMO = highest occupied molecular orbital). Therefore, we may assume that, as the energy of the lowest occupied orbital of the terminal O atom is lower than that of the terminal S atom, the possibly formed species $[(edt)_2Mo_2S_2(\mu\text{-}S)_2Cu_2(dppm)_2]$ and $[(edt)_2Mo_2S(\mu_3\text{-}S)(\mu\text{-}S)_2Cu_2(Py)_4]$ are prone to be easily oxidized into their oxygen analogues **3** and **4**, respectively.

The generation of symmetrical products in the cases of **3** and **4** prompted us to consider that a combination of both pyridine and diphosphine in the one compound may yield the desired asymmetric cluster. The reaction of **1** with 2 equiv of CuBr followed by the addition of a mixture of dppm and Py (molar ratio = 1:2) did generate an expected asymmetric cluster, **5**, as red crystals in 73% yield (Scheme 2). Unlike those observed in the preparations of **3** and **4**, the sulfur-to-oxygen transformation in **2** and **5** did not take place, which may be due to the fact that the terminal sulfurs of **1** all coordinate at copper(I) centers in the structures of **2** and **5**.

Solids **2**−**5** were relatively stable toward air and moisture. Cluster **2** is soluble in MeCN, dimethylsulfoxide (DMSO), and N,N-dimethylformamide (DMF), while **3**−**5** were insoluble in MeCN but soluble in CH_2Cl_2, $CHCl_3$, DMF, and

---

(9) (a) Shi, S.; Ji, W.; Tang, S. H.; Lang, J. P.; Xin, X. Q. *J. Am. Chem. Soc.* **1994**, *116*, 3615–3616. (b) Shi, S.; Ji, W.; Lang, J. P.; Xin, X. Q. *J. Phys. Chem.* **1994**, *98*, 3570–3572. (c) Lang, J. P.; Kawaguchi, H.; Ohnishi, S.; Tatsumi, K. *Chem. Commun.* **1997**, 405–406. (d) Lang, J. P.; Tatsumi, K. *Inorg. Chem.* **1998**, *37*, 160–162. (e) Lang, J. P.; Tatsumi, K. *Inorg. Chem.* **1998**, *37*, 6308–6316. (f) Lang, J. P.; Kawaguchi, H.; Tatsumi, K. *Chem. Commun.* **1999**, 2315–2316. (g) Yu, H.; Xu, Q. F.; Sun, Z. R.; Ji, S. J.; Chen, J. X.; Liu, Q.; Lang, J. P.; Tatsumi, K. *Chem. Commun.* **2001**, 2614–2615. (h) Lang, J. P.; Ji, S, J.; Xu, Q. F.; Shen, Q.; Tatsumi, K. *Coord. Chem. Rev.* **2003**, *241*, 47–60. (i) Lang, J. P.; Xu, Q. F.; Chen, Z. N.; Abrahams, B. F. *J. Am. Chem. Soc.* **2003**, *125*, 12682–12683. (j) Lang, J. P.; Xu, Q. F.; Yuan, R. X.; Abrahams, B. F. *Angew. Chem., Int. Ed.* **2004**, *43*, 4741–4745. (k) Lang, J. P.; Jiao, C. M.; Qiao, S. B.; Zhang, W. H.; Abrahams, B. F. *Inorg. Chem.* **2005**, *44*, 3664–3668. (l) Xu, Q. F.; Chen, J. X.; Zhang, W. H.; Ren, Z. G.; Li, H. X.; Zhang, Y.; Lang, J. P. *Inorg. Chem.* **2006**, *45*, 4055–4064. (m) Lang, J. P.; Xu, Q. F.; Zhang, W. H.; Li, H. X.; Ren, Z. G.; Chen, J. X.; Zhang, Y. *Inorg. Chem.* **2006**, *45*, 10487–10496. (n) Zhang, W. H.; Song, Y. L.; Ren, Z. G.; Li, H. X.; Li, L. L.; Zhang, Y.; Lang, J. P. *Inorg. Chem.* **2007**, *46*, 6647–6660. (o) Zhang, W. H.; Song, Y. L.; Zhang, Y.; Lang, J. P. *Cryst. Growth Des.* **2008**, *8*, 253–258. (p) Zhang, W. H.; Lang, J. P.; Zhang, Y.; Abrahams, B. F. *Cryst. Growth Des.* **2008**, *8*, 399–401. (q) Zhang, W. H.; Song, Y. L.; Wei, Z. H.; Li, L. L.; Huang, Y. J.; Zhang, Y.; Lang, J. P. *Inorg. Chem.* **2008**, *47*, 5332–5346.

(10) (a) Pan, W. H.; Chandler, T.; Enemark, J. H.; Stiefel, E. I. *Inorg. Chem.* **1984**, *23*, 4265–4269. (b) Bunzey, G.; Enemark, J. H. *Inorg. Chem.* **1978**, *17*, 682–688.

(11) (a) Zhu, N. Y.; Zheng, Y. F.; Wu, X. T. *J. Chem. Soc., Chem. Commun.* **1990**, 780–781. (b) Zhu, N. Y.; Zheng, Y. F.; Wu, X. T. *Inorg. Chem.* **1990**, *29*, 2705–2706.

(12) (a) Lin, P.; Wu, X. T.; Huang, Q.; Wang, Q. M.; Sheng, T. L.; Zhang, W. J.; Guo, J.; Lu, J. X. *Inorg. Chem.* **1998**, *37*, 5672–5674. (b) Lin, P.; Wu, X. T.; Zhang, W. J.; Guo, J.; Sheng, T. L.; Lu, J. X. *Chem. Commun.* **1997**, 1349–1350.

(13) (a) Bernholc, J.; Stiefel, E. I. *Inorg. Chem.* **1986**, *25*, 3876–3879. (b) Pan, W. H.; Harmer, M. A.; Halbert, T. R.; Stiefel, E. I. *J. Am. Chem. Soc.* **1984**, *106*, 459–460.

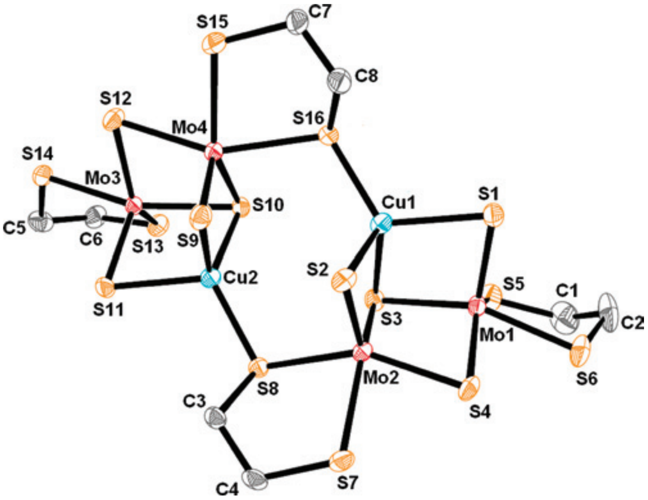

Figure 1. The dianion of **2** with 50% thermal ellipsoids. A pseudo 2-fold axis, perpendicular to the page, runs between the two incomplete cubane units. All hydrogen atoms are omitted for clarity.

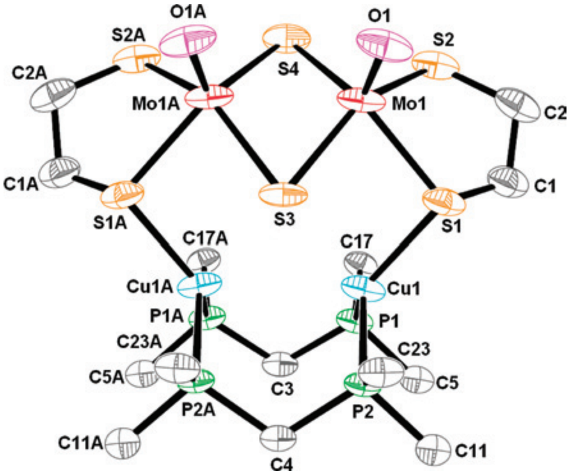

Figure 2. Molecular structure of **3** with 50% thermal ellipsoids. For clarity, all hydrogen atoms are omitted and all phenyl groups are represented by their ipso carbon atoms. Symmetry code: A, x, $1/2 - y$, z.

DMSO. The elemental analyses were consistent with their chemical formulas. In the IR spectra of **2**−**5**, bands at 497/470/439 (**2**), 470/431 (**3**), 472/449 (**4**), and 487/470/437 (**5**) cm^{-1} were assigned as the bridging Mo−S stretching vibrations. In addition, the IR spectra of **3** and **4** indicated the characteristic terminal Mo═O stretching bands at about 933 cm^{-1}. The electronic spectra of **2**−**5** are characterized by three absorptions at a range of 228−506 nm. Bands at 325 (**2**), 318 (**3**), 336 (**4**), and 318 (**5**) are slightly red-shifted relative to that of the precursor **1** at 306 nm. These bands are probably dominated by the S ↔ Mo(V) charge transfers in the $[Mo_2O_xS_{4-x}]$ ($x = 0-2$) moieties. The ^1H NMR spectrum of **2** at CD_3CN at ambient temperature showed a quadruplet for ethylene group at 3.54−3.52 ppm. The ^1H NMR spectra in $CDCl_3$ at ambient temperature showed correct phenyl/methylene/ethylene (**3**) and pyridyl/ethylene (**4**) proton ratios. The ^1H NMR spectrum of **5** in DMSO-d_6 exhibited a doublet and two quadruplets for the pyridyl group at 8.55−8.54 ppm, 7.36−7.34 ppm, and 7.78−7.76 ppm; a singlet for the phenyl group at 7.61 ppm; a quadruplet for the ethylene groups of edt at 3.55−3.54 ppm; and a singlet for the methylene group of dppm at 3.15 ppm. The identities of **2**−**5** were further confirmed by X-ray crystallography.

Crystal Structure of $[Et_4N]_2[(edt)_2Mo_2(\mu\text{-}S)_3(\mu_3\text{-}S)Cu]_2 \cdot 2CH_2Cl_2$ ($2 \cdot 2CH_2Cl_2$). An X-ray crystallographic analysis revealed that $2 \cdot 2CH_2Cl_2$ crystallizes in the triclinic space group $P\bar{1}$, and the asymmetric unit contains one discrete $[(edt)_2Mo_2(\mu\text{-}S)_3(\mu_3\text{-}S)Cu]_2^{2-}$ dianion, two Et_4N^+ cations, and two CH_2Cl_2 solvent molecules. The cluster dianion consists of two chemically similar $[Mo_2(\mu\text{-}S)_3(\mu_3\text{-}S)(edt)_2Cu]^-$ anions linked by two strong Cu−S_{edt} bonds (Figure 1). Such a $[Mo_4S_8Cu_2]$ cluster core is unprecedented in the chemistry of $[MS_4]^{2-}$, $[(\eta^5\text{-}C_5Me_5)MS_3]^-$, and $[M_2S_4]^{2-}$ (M = Mo, W). Each half of the dianion ($[Mo_2(\mu\text{-}S)_3(\mu_3\text{-}S)(edt)_2Cu]^-$) can be related to the incomplete cubanelike structure of type b (Scheme 1). The cluster depicted in type b possesses a mirror plane, but the asymmetry introduced as a result of one S_{edt} bridging to the other half of the dimer leads to the generation of a trinuclear unit with asymmetry at each of the metal centers clearly apparent. The dimeric halves are not related by symmetry, but there is a pseudo 2-fold axis that passes through the dianion. The two halves have the same absolute configuration, making each dimeric anion chiral. The dimers crystallize in a centrosymmetric space group, and thus each crystal contains a racemic mixture of the dimeric enantiomers.

In the structure of the dianion of **2**, the formal oxidation states for each of the Mo and Cu atoms are assumed to be +5 and +1, respectively. Each Mo center adopts a distorted square-pyramidal geometry, coordinated by two S_{edt}, one μ_3-S, and two μ-S atoms (Mo1 and Mo3) or by one S_{edt}, one μ-S_{edt}, one μ_3-S, and two μ-S atoms (Mo2 and Mo4). Each Cu atom is coordinated by one μ-S_{edt}, one μ_3-S, and two μ-S atoms, forming a distorted tetrahedron coordination geometry. As shown in Table 1, the mean Mo−μ-S (2.159(2) Å) and Mo−μ_3-S (2.342(2) Å) bond lengths of **2** are elongated by 0.05 Å relative to those of the corresponding ones of **1** due to its coordination to a Cu center.[10a] The mean Mo−μ-S_{edt}(8, 16) distance (2.453(2) Å) is longer than that of the Mo−S_{edt} bonds (2.377(2) Å) as a consequence of S8 and S16 binding to Cu atoms. The mean Mo···Mo separation (2.8525(14) Å) is similar to those of **1** (2.863(3) Å) and $[Et_4N]_2[Mo_2Cu_2(\mu_3\text{-}S)_4(PPh_3)_2(edt)_2]$ (2.858(3) Å)[11a] but longer than those of $[(dtc)_2Mo_2(\mu_3\text{-}S)(\mu\text{-}S)_3(CuBr)_n]$ (av. 2.7982(9) Å for $n = 1$; av. 2.766(2) Å for $n = 2$).[14] The average Mo···Cu contact of 2.7711(14) Å is close to those of $[(dtc)_2Mo_2(\mu_3\text{-}S)(\mu\text{-}S)_3(CuBr)_n]$ (av. 2.769(2) Å for $n = 1$; 2.788(3) Å for $n = 2$). The mean Cu−μ-S_{edt} bond length (av. 2.226(2) Å) is shorter than those of Cu(1)−μ-S (2.370(3) Å) and Cu(1)−μ_3-S_{br} bonds (av. 2.291(2) Å).

Crystal Structure of $[(edt)_2Mo_2O_2(\mu\text{-}S)_2Cu_2(dppm)_2]$ (3). Compound **3** crystallizes in the orthorhombic space group *Pnma*, and its asymmetric unit contains half of the $[(edt)_2Mo_2O_2(\mu\text{-}S)_2Cu_2(dppm)_2]$ molecule. As depicted in Figure 2, **3** may be considered as having a $[(edt)_2Mo_2O_2(\mu\text{-}S)_2]^{2-}$ unit bound to a $[Cu_2(dppm)_2]^{2+}$ cation through a pair of Cu−μ-S_{edt} bonds (type c in Scheme 1). A crystallographic mirror plane runs

---

(14) Wei, Z. H.; Xu, Q. F.; Li, H. X.; Chen, J. X.; Lang, J. P. *J. Organomet. Chem.* **2003**, *87*, 197–202.

Table 1. Selected Bond Distances (Å) for **2**·$2CH_2Cl_2$, **3**, **4**, and **5**·Py

Compound **2**·$2CH_2Cl_2$			
Mo(1)···Mo(2)	2.8569(13)	Mo(3)···Mo(4)	2.8480(15)
Mo(1)···Cu(1)	2.7843(14)	Mo(2)···Cu(1)	2.7760(15)
Mo(3)···Cu(2)	2.7704(16)	Mo(4)···Cu(2)	2.7539(15)
Mo(1)−S(1)	2.176(2)	Mo(1)−S(4)	2.306(3)
Mo(1)−S(3)	2.376(2)	Mo(1)−S(5)	2.386(3)
Mo(1)−S(6)	2.396(2)	Mo(2)−S(2)	2.148(2)
Mo(2)−S(4)	2.329(2)	Mo(2)−S(3)	2.339(2)
Mo(2)−S(7)	2.385(2)	Mo(2)−S(8)	2.450(2)
Cu(1)−S(16)	2.230(2)	Cu(1)−S(3)	2.303(2)
Cu(1)−S(1)	2.346(3)	Cu(1)−S(2)	2.408(3)
Cu(2)−S(8)	2.221(2)	Cu(2)−S(10)	2.279(2)
Cu(2)−S(11)	2.333(2)	Cu(2)−S(9)	2.393(3)
Compound **3**			
Mo(1)···Mo(1A)	2.8726(15)	Mo(1)−O(1)	1.714(4)
Mo(1)−S(4)	2.3248(18)	Mo(1)−S(3)	2.3660(17)
Mo(1)−S(2)	2.392(2)	Mo(1)−S(1)	2.459(2)
Cu(1)−S(1)	2.3047(18)	Cu(1)−S(3)	2.6042(19)
Cu(1)−P(1)	2.2414(16)	Cu(1)−P(2)	2.2847(15)
Compound **4**			
Mo(1)···Mo(2)	2.8752(8)	Mo(1)···Cu(1)	2.7717(10)
Mo(1)···Cu(2)	2.7147(8)	Mo(1)−S(3)	2.2194(13)
Mo(1)−S(4)	2.3062(12)	Mo(1)−S(5)	2.3199(12)
Mo(1)−S(2)	2.4178(12)	Mo(1)−S(1)	2.4374(12)
Cu(1)−N(1)	2.059(4)	Cu(1)−S(3)	2.2663(13)
Cu(1)−S(1)	2.2830(13)		
Compound **5**·Py			
Mo(1)···Mo(2)	2.8429(9)	Mo(1)···Cu(1)	2.7700(10)
Mo(2)···Cu(1)	2.8073(10)	Mo(2)···Cu(2)	2.7995(10)
Mo(3)···Mo(4)	2.8583(9)	Mo(3)···Cu(3)	2.7520(13)
Mo(4)···Cu(3)	2.7972(11)	Mo(4)···Cu(4)	2.8318(12)
Mo(1)−S(3)	2.1621(16)	Mo(1)−S(2)	2.3106(16)
Mo(1)−S(1)	2.3532(18)	Mo(1)−S(7)	2.3714(17
Mo(1)−S(8)	2.3932(19)	Mo(2)−S(4)	2.2030(16)
Mo(2)−S(2)	2.3102(18)	Mo(2)−S(1)	2.3592(15)
Mo(2)−S(6)	2.3689(17)	Mo(2)−S(5)	2.4078(18)
Mo(3)−S(13)	2.1595(18)	Mo(3)−S(10)	2.3121(18)
Mo(3)−S(9)	2.3493(18)	Mo(3)−S(16)	2.384(2)
Mo(3)−S(15)	2.393(2)	Mo(4)−S(14)	2.2079(17)
Mo(4)−S(10)	2.3193(19)	Mo(4)−S(9)	2.3388(16)
Mo(4)−S(11)	2.3636(17)	Mo(4)−S(12)	2.4258(18)
Cu(1)−P(1)	2.2215(17)	Cu(1)−S(1)	2.2867(17)
Cu(1)−S(3)	2.3507(18)	Cu(1)−S(4)	2.3904(16)
Cu(2)−N(1)	2.074(3)	Cu(2)−P(2)	2.2898(18)
Cu(2)−S(5)	2.2955(19)	Cu(2)−S(4)	2.3293(19)
Cu(3)−P(4)	2.2120(18)	Cu(3)−S(9)	2.2820(17)
Cu(3)−S(13)	2.341(2)	Cu(3)−S(14)	2.3744(17)
Cu(4)−N(2)	2.096(4)	Cu(4)−S(12)	2.2954(19)
Cu(4)−P(3)	2.2979(19)	Cu(4)−S(14)	2.3206(18)

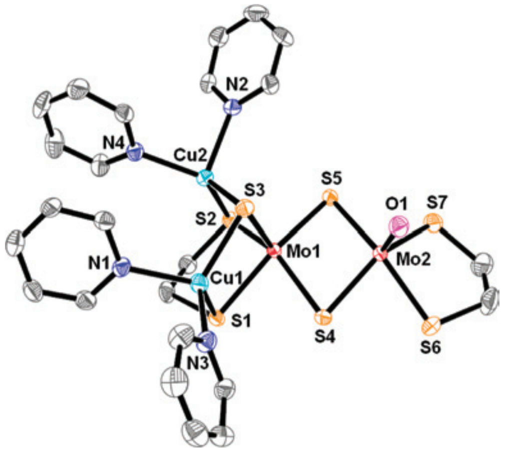

Figure 3. Molecular structure of **4** with 50% thermal ellipsoids. All hydrogen atoms are omitted for clarity.

through S3, S4, C3, and C4 atoms. Each Mo center adopts a distorted square-pyramidal geometry, coordinated by one terminal O$_t$, one S$_{edt}$, one μ-S$_{edt}$, and two μ-S atoms. Each Cu center adopts an approximately trigonal-planar coordination geometry coordinated by one μ-S$_{edt}$ and two P atoms from two dppm ligands. The Cu center sits out of the plane of these three donor atoms by 0.51 Å. The Cu1 and Cu1A atom also forms a longer bond to atom S3 (2.6042(18) Å) that sits on the mirror plane that passes through the cluster. The eight-membered [Cu−P−C−P−Cu−P−C−P] ring in the $[Cu_2(dppm)_2]^{2+}$ dication adopts a boat conformation. The Mo···Mo contact in **3** is longer than those of **1** and **2**·$2CH_2Cl_2$ (Table 1). The Mo−μ-S$_{edt}$ bond length is elongated by 0.053 Å relative to those of Mo−S$_{edt}$ as a consequence of μ-S$_{edt}$ coordination to a M atom. In addition, the Mo−S3 bond length is slightly enlongated relative to that of the Mo−S2 bond length due to the weak coordination of S3 at M centers. The mean Cu−μ-S$_{edt}$ distance (2.3047(18) Å) is longer than that of **2**·$2CH_2Cl_2$ due to the existence of bulky dppm ligands. The Cu−P and Mo−O$_t$ bond lengths are normal.

Crystal Structure of [(edt)$_2$Mo$_2$O(μ_3-S)(μ-S)$_2$Cu$_2$(Py)$_4$] (4). Cluster **4** crystallizes in the monoclinic space group *Cc*, and its asymmetric unit consists of a single [(edt)$_2$Mo$_2$O(μ_3-S)(μ-S)$_2$Cu$_2$(Py)$_4$] cluster. This molecule may be considered as a $[(edt)_2Mo_2OS(\mu\text{-}S)_2]^{2-}$ moiety linked to a pair of $[Cu(Py)_2]^+$ fragments through three sulfur atoms, S1, S2, and S3, all of which are coordinated to the same Mo center (Mo1; Figure 3). Although **4** lacks the internal symmetry present in **3**, the cluster core does possess pseudomirror symmetry. Mo1 is coordinated by one μ_3-S, two μ-S, and two μ-S$_{edt}$ atoms, while Mo2 is coordinated by one terminal O, two S$_{edt}$, and two μ-S atoms, forming a distorted square-pyramidal geometry. The tetrahedral coordination environment of each Cu center is completed by two μ-S$_{edt}$ atoms from one edt and two N atoms from a pair of Py ligands. The Mo···Mo separation is close to that of **3**, but slightly longer than **2**. Compared with the corresponding ones of **2**, the mean Mo···Cu distance at 2.7432(8) Å is slightly reduced by 0.05 Å (Table 1). The mean Mo−μ-S$_{edt}$ distance (2.4276(12) Å) is shorter than that of **2** (2.453(2) Å), while the mean Mo−S$_{edt}$ distance (2.4114(14) Å) is longer than that of **2** (2.377(2) Å). The Mo2−O1 distance is close to that in **3** but shorter than those in [EtN$_4$]$_2$[{(edt)$_2$Mo$_2$S$_2$O$_2$Cu$_2$}$_3$(μ_6-S)$_2$] (av. 1.777 Å).[11a] The mean Cu−μ-S$_{edt}$ bond length (av. 2.2731(12) Å) is between those of **2** and **3**. The average Mo−μ-S, Mo−μ_3-S$_{br}$, Cu−μ_3-S$_{br}$, and Cu−N bond lengths are normal.

Crystal Structure of [(edt)$_2$Mo$_2$(μ-S)$_2$(μ_3-S)$_2$Cu$_2$(dppm)(Py)]·Py (5·Py). Compound **5**·Py crystallizes in the monoclinic space group *P*2$_1$, and the asymmetric unit consists of two crystallographically independent, but chemically similar, [(edt)$_2$Mo$_2$(μ-S)$_2$(μ_3-S)$_2$Cu$_2$(dppm)(Py)] clusters in addition to a pair of pyridine solvent molecules. The following description refers specifically to the cluster that includes Mo(1) and Mo(2). As in the case of **2**−**4**, the Mo$_2$S$_4$(edt)$_2$ cluster associates with a pair of Cu(I) centers, Cu1 and Cu2 (Figure 4a). Each Mo center adopts a distorted square-pyramidal geometry, coordinated by two S$_{edt}$, one μ_3-S, and

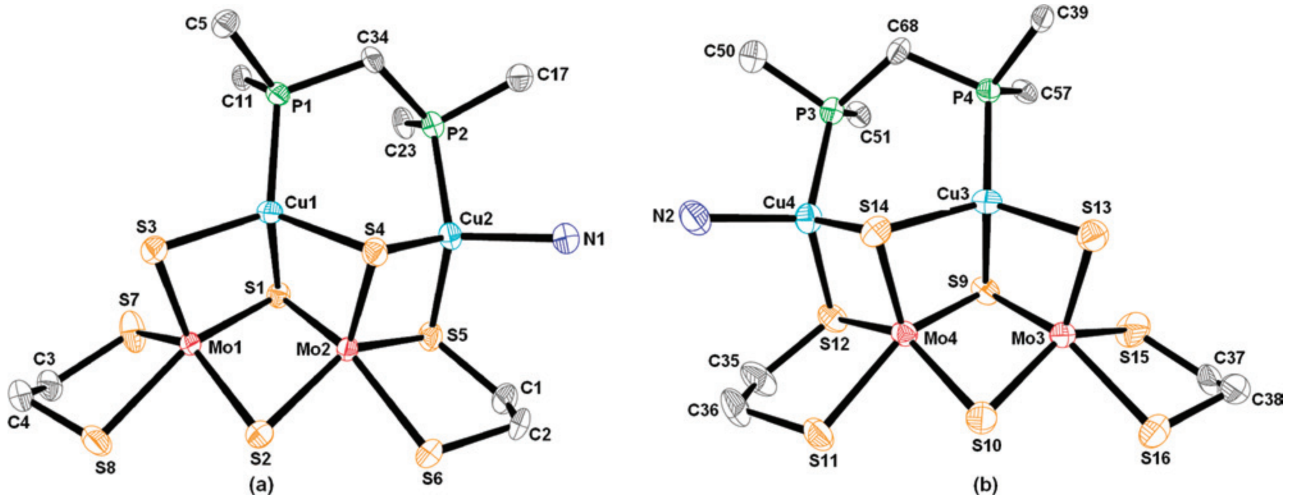

Figure 4. Molecular structure and labeling of **5** with 50% thermal ellipsoids. For clarity, all hydrogen atoms are omitted and all pyridyl or phenyl groups are represented by their ipso nitrogen or carbon atoms.

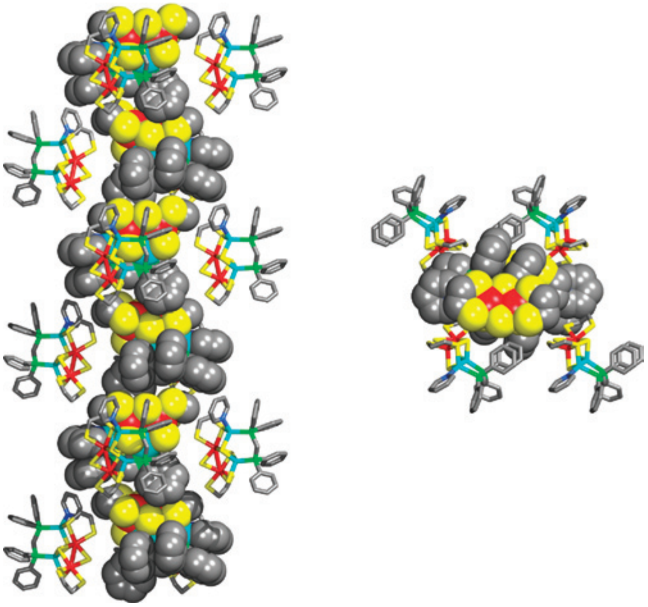

Figure 5. Side view (left) and top view (right) of the helical packing along a 2_1 axis. The first cluster is indicated by the space-filling representation, while the second type is indicated by the rod representation.

two μ-S atoms (Mo1) or by one S_{edt}, one μ-S_{edt}, one μ-S, and two μ_3-S atoms (Mo2). Each Cu center adopts an approximately trigonal-planar coordination geometry coordinated by one μ-S_{edt} and two P atoms from two dppm ligands. Cu1 is bound to three sulfur donors that result in the formation of an incomplete cubane unit involving both Mo centers. A tetrahedral environment for Cu(I) is completed by a single phosphorus atom belonging to a bridging diphosphine. Atom Cu2 associates with a pair of S atoms that are only bound to Mo2. The incorporation of this second Cu center leads to the introduction of asymmetry in the metal−sulfur core. The asymmetric environment of Cu2 is completed by a pyridyl N atom and the second P atom belonging to the bridging dppm ligand. This cluster is arranged around a 2-fold screw axis that runs parallel to the *b* axis (see Figure 5).

The second type of cluster in this crystal structure (Figure 4b) is not related to the first by crystal symmetry; however, a comparison of part a with part b of Figure 4 reveals that they are enantiomeric forms of the same cluster. This leads to an unusual situation where a crystal contains an enantiomeric pair but with the pair not related by crystal symmetry. The second cluster is arranged around 2-fold screw axes parallel to the *b* axis but different axes from those that the first cluster is situated around. Sheets of the second cluster extend in the *a*−*b* plane and are separated by parallel sheets of the first cluster. It is assumed that the bulk product contains a "racemic mixture of crystals"; that is, there are crystals where each of the crystallographically unique clusters will be of opposite hand to that found in the reported structure.

As shown in Table 1, the bond lengths and angles of the two independent clusters in **5**·Py are different. The Mo1···Mo2 contact is slightly shorter than the Mo3···Mo4 contact. Their mean value (2.8506(9) Å) is close to that in **2**, but shorter than those of **3** and **4**. In Figure 4a, the Mo2···Cu1 and Mo2···Cu2 contacts are similar, but longer than the Mo1···Cu1 contact. In Figure 4b, the Mo4···Cu3 separation is longer than the Mo3···Cu3 separation, but shorter than the Mo4···Cu4 separation. The mean Mo···Cu separation at 2.7930(12) Å of **5** is longer than those of **2**−**4**. The mean Mo4−S12 separation is longer than the Mo2−S5 separation. Their mean Mo−μ-S_{edt} contact (2.4168(18) Å) is shorter than that of **2** and **4**. In both clusters of **5**, the Cu−μ-S_{edt} bond lengths are almost the same, and their mean value (2.2955(19) Å) is longer than those of **2** and **4**. The average Mo−S_{edt}, Mo−μ-S, Mo−μ_3-S_{br}, Cu−μ_3-S_{br}, Cu−P, and Cu−N bond lengths are normal.

Conclusion

In this work, we have demonstrated that an asymmetric dimeric cluster, **2**, was generated by combining **1** with equimolar CuBr. When 2 equiv of CuBr are added, an insoluble precipitate is formed, which can be dissolved by the addition of ligands (dppm and Py) that are able to act as strong donors toward Cu(I). As anticipated, both **3** and **4** contain a pair of Cu(I) centers. Each of these clusters has internal mirror symmetry or pseudo mirror symmetry. Through the addition of a mixture of dppm and Py ligands,

Table 2. Crystallographic Data for **2**·$2CH_2Cl_2$, **3**, **4**, and **5**·Py

	2·$2CH_2Cl_2$	**3**	**4**	**5**·Py
formula	$C_{26}H_{60}N_2Mo_4Cu_2S_{16}Cl_4$	$C_{54}H_{52}Cu_2Mo_2O_2P_4S_6$	$C_{24}H_{28}Cu_2Mo_2N_4OS_7$	$C_{39}H_{40}N_2Mo_2S_8Cu_2P_2$
fw	1566.54	1368.24	931.97	1174.21
cryst syst	triclinic	orthorhombic	monoclinic	monoclinic
space group	$P\bar{1}$	*Pnma*	*Cc*	$P2_1$
a (Å)	12.235(2)	22.196(4)	9.6843(19)	12.594(3)
b (Å)	14.633(3)	20.525(4)	17.934(4)	20.877(4)
c (Å)	16.959(3)	12.165(2)	18.418(4)	17.576(4)
α (deg)	84.44(3)			
β (deg)	80.71(3)	94.26(3)	106.06(3)	
γ(deg)	65.45(3)			
V(Å^3)	2724.0(11)	5542.0(17)	3190.0(12)	4440.8 (18)
D_{calcd} (g cm^{-3})	1.910	1.640	1.940	1.756
Z	2	4	4	4
μ (mm^{-1})	2.49	1.58	2.57	1.98
F(000)	1560	2760	1848	2352
total reflns	27564	35644	10196	35802
unique reflns	12293 ($R_{int} = 0.0569$)	5226 ($R_{int} = 0.0995$)	4606 ($R_{int} = 0.0246$)	15639 ($R_{int}= 0.0384$)
obsd reflns	10096 ($I > 2\sigma(I)$)	4698 ($I > 2\sigma(I)$)	4561 ($I > 2\sigma(I)$)	14944 ($I > 2\sigma(I)$)
no. of variables	477	338	361	890
R^a	0.0854	0.0632	0.0231	0.0415
wR^b	0.1289	0.1387	0.0532	0.0910
GOF^c	1.205	1.190	1.068	1.058
$\Delta\rho_{max}$ (e Å^{-3})	2.533	1.340	0.701	1.147
$\Delta\rho_{min}$ (e Å^{-3})	−1.405	−1.040	−0.383	−0.932

[a] $R_1 = |F_o|$. [b] $wR_2 = \{w(|F_o| - |F_c|)^2/w|F_o|^2\}\}^{1/2}$. [c] GOF $= \{w(|F_o| - |F_c|)^2/(n - p)\}^{1/2}$, where n is the number of reflections and p is total number of parameters refined.

as in the case of the formation of **5**, we have succeeded in introducing asymmetry into the cluster. Although we have been able to generate asymmetric clusters in the cases of **2** and **5**, the products are racemic. Nevertheless, the approach of using mixed ligands to encourage the generation of asymmetric species for such systems may be worth developing in attempts to generate enantiomerically pure products involving Mo/M/S clusters.

Experimental Section

General Procedures. The cluster precursor, **1**, was prepared according to the literature method.[10a] All solvents were predried over activated molecular sieves and refluxed over the appropriate agents under argon. Other chemicals and reagents were obtained from commercial sources and used as received. The elemental analyses for C, H, and N were performed on a Carlo-Erba CHNO-S microanalyzer. IR spectra were recorded on a Varian 1000 FT-IR spectrometer as KBr disks (4000−400 cm^{-1}). ^{1}H NMR spectra were recorded at ambient temperature on a Varian UNITY-400 spectrometer. The ^{1}H NMR chemical shifts are reported relative to TMS in CD_3CN, $CDCl_3$, and DMSO-d_6. UV−vis spectra were measured on a Varian 50 UV−visible spectrophotometer.

$[Et_4N]_2[(edt)_2Mo_2(\mu\text{-}S)_3(\mu_3\text{-}S)Cu]_2\cdot 2CH_2Cl_2$ (2·$2CH_2Cl_2$). To a solution of **1** (76 mg, 0.1 mmol) in 20 mL of CH_2Cl_2 was added dropwise a solution of CuBr (15 mg, 0.1 mmol) in 20 mL of MeCN. The mixed solution turned to dark red immediately. After being stirred at room temperature for 1 h, the resulting solution was filtered. Diethyl ether (30 mL) was carefully layered onto the filtrate to form red crystals of **2**·$2CH_2Cl_2$ in four days, which were collected by filtration and washed with Et_2O and dried in the air. Yield: 47 mg (60% based on Mo). Anal. calcd for $C_{26}H_{60}Cl_4Cu_2Mo_4N_2S_{16}$: C, 19.93; H, 3.86; N, 1.79. Found: C, 19.65; H, 3.98; N, 1.89. IR (KBr disk): 2970 (m), 2893 (s), 2812 (w), 1616 (w), 1477 (s), 1454 (s), 1412 (s), 1385 (s), 1269 (s), 1234 (m), 1169 (m), 1030 (w), 999 (m), 933 (w), 829 (w), 783 (m), 497 (s), 470 (s), 439 (m) cm^{-1}. UV−vis (MeCN) (λ_{max}/nm (ε/M^{-1}cm^{-1})): 228 (84700), 325 (36100), 465 (910). ^{1}H NMR (CD_3CN, 400 MHz): δ 3.54−3.52 (q, 8H, SCH_2CH_2S), 3.34−3.25 (m, 8H, CH_2CH_3), 1.25−1.22 (m, 12H, CH_2CH_3).

$[(edt)_2Mo_2O_2(\mu\text{-}S)_2Cu_2(dppm)_2]$ (3). To a solution of **1** (76 mg, 0.1 mmol) in 10 mL of CH_2Cl_2 was added dropwise a solution of CuBr (29 mg, 0.2 mmol) in 20 mL of MeCN. A great quantity of dark red precipitate was formed within seconds. The red slurry was stirred for 10 min, and a solution of dppm (79 mg, 0.2 mmol) in CH_2Cl_2 (10 mL) was added. The resulting mixture was stirred for another 30 min, forming a homogeneous red solution. The addition of MeOH into this solution yielded a red microcrystalline solid, which was collected by filtration, washed with MeCN and Et_2O, and dried *in vacuo*. Recrystallization of the solid in DMF/*i*-PrOH afforded red crystals of **3** two days later. Yield: 73 mg (50% based on Mo). Anal. calcd for $C_{54}H_{52}Cu_2Mo_2O_2P_4S_6$: C, 47.40; H, 3.83. Found: C, 47.20; H, 3.68. IR (KBr disk): 1481 (m), 1434 (m), 1270 (w), 1096 (m), 994 (w), 933 (s), 737 (s), 692 (s), 502 (m), 470 (m), 431 (w) cm^{-1}. UV−vis (DMF) (λ_{max}/nm (ε/M^{-1}cm^{-1})): 232 (61800), 318 (28200), 508 (9000). ^{1}H NMR ($CDCl_3$, 400 MHz): δ 7.52 (m, 40H, Ph), 3.51−3.49 (m, 8H, SCH_2CH_2S), 3.46 (m, 8H, PCH_2P).

$[(edt)_2Mo_2O(\mu_3\text{-}S)(\mu\text{-}S)_2Cu_2(Py)_4]$ (4). To a red suspension of **1** (38 mg 0.05 mmol) and CuBr (15 mg 0.1 mmol) in 10 mL of CH_2Cl_2/MeCN was added 10 mL of pyridine. The mixture was stirred for 2 h at room temperature and filtered. Slow evaporation of the solvents from the filtrate gave rise to dark red crystals of **4** one week later. Yield: 35 mg (70% based on Mo). Anal. calcd for $C_{24}H_{28}Cu_2Mo_2N_4OS_7$: C, 30.93; H, 3.02; N, 6.01. Found: C, 31.21; H, 3.22; N, 6.36. IR (KBr disk): 2891 (w), 1594 (w), 1482 (w), 1440 (s), 1270 (w), 1234 (w), 1214 (w), 1065 (m), 1035 (m), 933 (s), 748 (m), 740 (m), 694 (s), 472 (w), 449 (w) cm^{-1}. UV−vis (DMF) (λ_{max}/nm (ε/M^{-1}cm^{-1})): 242 (69300), 336 (25600), 525 (7900). ^{1}H NMR ($CDCl_3$, 400 MHz): δ 8.55−8.54, 7.82−7.75, 7.41−7.37 (m, 5 H, Py), 3.65−3.56 (m, 8 H, SCH_2CH_2S).

$[(edt)_2Mo_2(\mu\text{-}S)_2(\mu_3\text{-}S)_2Cu_2(dppm)(Py)]\cdot Py$ (5·Py). To a suspension of **1** (76 mg, 0.1 mmol) and CuBr (29 mg, 0.2 mmol) in 10 mL of CH_2Cl_2/MeCN was added dppm (38 mg, 0.1 mmol) and pyridine (16 mg, 0.2 mmol). The mixture was stirred at room temperature for 30 min, forming a dark red homogeneous solution.

Et_2O (5 mL) was carefully layered onto the resulting solution to afford dark red crystals of **5**·Py, which were collected by filtration and washed with CH_2Cl_2/Et_2O (v/v = 1:5) and dried in the air. Yield: 82 mg (73% based on Mo). Anal. calcd for $C_{39}H_{40}Cu_2Mo_2N_2P_2S_8$: C, 39.89; H, 3.43; N, 2.39. Found: C, 40.08; H, 3.61; N, 2.62. IR (ν cm^{-1}): 2899 (w), 2813 (w), 1596 (w), 1581 (w), 1481 (m), 1434 (s), 1413 (w), 1273 (m), 1184 (w), 1098 (m), 1066 (w), 998 (w), 773 (m), 739 (s), 696 (s), 516 (m), 487 (m), 470 (m), 437 (w) cm^{-1}. UV−vis (DMF) (λ_{max}/nm (ε/$M^{-1}cm^{-1}$)): 236 (65100), 318 (26500), 505 (9500). ^1H NMR (DMSO-d_6, 400 MHz): δ 8.55−8.54 (d, 1H, Py), 7.77−7.76 (dq, 2H, Py), 7.36−7.34 (dq, 2H, Py), 7.37 (m, 20 H, Ph), 3.55−3.54 (q, 8H, SCH_2CH_2S), 3.16 (s, 2H, PCH_2P).

X-Ray Structure Determination. X-ray-quality crystals of **2**−**5** were obtained directly from the above preparation. All measurements were made on a Rigaku Mercury CCD X-ray diffractometer (3 kW) by using graphite monochromated Mo Kα (λ = 0.71073 Å). Single crystals of **2**−**5** were mounted with grease at the top of a glass fiber and cooled at 193 K in a liquid-nitrogen stream. Cell parameters were refined by using the program *CrystalClear* (Rigaku and MSC, version 1.3, 2001). The collected data were reduced by using the program *CrystalClear*, and an absorption correction (multiscan) was applied. The reflection data were also corrected for Lorentz and polarization effects.

The crystal structures of **2**−**5** were solved by direct methods and refined on F^2 by full-matrix least-squares methods with the *SHELXL-97* program.[15] For **3**, C26−C28 of one phenyl group were split into two positions with an occupancy factor of 0.514/0.496. For **5**·Py, C3, C4, C37, and C38 of the two edt ligands were found to be disordered over two positions with 0.59/0.41 occupancy. All non-H atoms were refined anisotropically. All H atoms were placed in geometrically idealized positions (C−H = 0.98 Å, with U_{iso}(H) = 1.5U_{eq}(C) for methyl groups; C−H = 0.99 Å, with U_{iso}(H) = 1.2U_{eq}(C) for methylene groups; C−H = 0.95 Å, with U_{iso}(H) = 1.2U_{eq}(C) for aromatic rings) and constrained to ride on their parent atoms. A summary of the key crystallographic information for **2**−**5** is listed in Table 2.

Acknowledgment. This work was financially supported by the National Natural Science Foundation of China (Grant Nos. 20525101 and 20871088), the Specialized Research Fund for the Doctoral Program of Higher Education (Grant No. 20050285004), the State Key Laboratory of Organometallic Chemistry of Shanghai Institute of Organic Chemistry (2008-25), and the "SooChow Scholar" Program and Program for Innovative Research Team of Suzhou University. The authors also thank Prof. J. L. Zou at NanJing University for his help in measuring the circular dichroism of **5**. We are grateful to the reviewers and editors for their helpful suggestions.

Supporting Information Available: Crystallographic data of compounds **2**−**5** (CIF). This material is available free of charge via the Internet at http://pubs.acs.org.

IC801100G

---

(15) Sheldrick, G. M. *SHELXS97*; *SHELXL97*; University of Göttingen: Göttingen, Germany, 1997.